



Microstructural transition and densification behavior of modified soil: a quantitative SEM study

 Assel Tulebekova¹,  Natalya Ryvkina¹,  Dauren Yessentay^{2,*},  Akmaral Yeleussinova¹

¹Department of Civil Engineering, L.N. Gumilyov Eurasian National University, Astana, Kazakhstan

²Department of Transportation Engineering and Building Materials Production, L.B. Goncharov Kazakh Automobile and Road Institute, Almaty, Kazakhstan

*Correspondence: yessentaydauren063@gmail.com

Abstract: This study investigates the microstructural transition and densification behavior of soil modified by xanthan gum (XG) using quantitative scanning electron microscopy (SEM) analysis. Soil specimens were prepared with 0%, 3%, 6%, and 9% XG content. SEM images were processed using image analysis techniques to determine the solid area fraction and characteristic particle size parameters. A densification index was introduced to quantify the ratio between solid and pore phases within the observed microstructure. The results reveal a non-monotonic structural evolution with increasing polymer content. The solid area fraction reached its maximum at 3%, indicating the most pronounced local densification of the particle structure within the analyzed micrographs. At 6%, a reduction in densification was observed, reflecting a change in particle packing configuration and the development of a more heterogeneous microstructural arrangement. At 9%, partial recovery of structural continuity occurred, accompanied by evidence of polymer agglomeration and spatial heterogeneity. Based on quantitative metrics and microstructural observations, three structural stages were identified: discrete particle stage, bridged stage, and matrix-dominated stage. The findings demonstrate that XG dosage significantly influences soil microstructure in a nonlinear manner. This SEM-based approach provides a systematic framework for identifying microstructural transitions in biopolymer-modified soils.

Keywords: xanthan gum, soil stabilization, microstructural transition, scanning electron microscopy, densification index.

1. Introduction

Soil stabilization is widely applied in geotechnical engineering to enhance the mechanical and hydraulic performance of problematic soils. Conventional stabilization techniques commonly involve cement or lime; however, these additives may significantly increase environmental impact and alter soil chemistry. In response to sustainability concerns, polymer-based treatments have attracted growing attention as an alternative ground improvement strategy [1].

Polymers interact with soil particles primarily through physicochemical mechanisms, including surface coating, interparticle bonding, and partial pore filling [2]. These interactions can alter particle packing and modify the internal microstructure without forming rigid cementitious bonds [3]. The resulting structural changes depend strongly on polymer concentration and distribution within the soil matrix. Therefore, quantitative evaluation of microstructural modifications is essential for understanding the mechanisms governing polymer-stabilized soils. Natural biopolymers such as chitosan, xanthan gum (XG), guar gum, carboxymethylcellulose, alginates, and modified starches, as well as their mixed compositions, are used as polymeric soil stabilizers, forming a spatial binding matrix in the pore space of the soil [4]. Among various biopolymers, XG has been extensively investigated for its ability to enhance soil strength and modify plasticity characteristics. Experimental studies [5] demonstrated that XG treatment increases compressive strength and cohesion, with performance strongly dependent on polymer dosage and curing conditions. Durability evaluations

under cyclic wetting-drying further showed that treated soils generally retain higher residual strength than untreated materials, highlighting the practical potential of XG for geotechnical applications.

The influence of environmental weathering on biopolymer-treated soils has also been systematically examined. [6] investigated the effects of cyclic wetting-drying (W-D) and freezing-thawing (F-T) on strength durability and reported that repeated cycles gradually reduced soil strength due to water adsorption and localized dilution of the biopolymer matrix. Poorly graded sands were found to be more vulnerable to degradation; however, the presence of 15-25% fines significantly improved resistance to weathering.

Despite progressive strength loss, treated soils maintained sufficient durability under multiple W-D and F-T cycles, supporting their suitability for slope reinforcement applications. From a mechanistic perspective, XG acts as a biodegradable polysaccharide that interacts with soil particles through physicochemical bonding. [3] demonstrated that XG forms rigid matrix-like structures between uncharged grains while interacting with charged clay surfaces, thereby enhancing interparticle bonding and overall stability. The reinforcement efficiency was shown to be highest in well-graded soils containing fine particles and was governed by several key parameters, including soil type, moisture content, biopolymer concentration, and mixing method. These findings underline the importance of optimizing mixture design to achieve maximum performance.

Beyond laboratory-scale assessments, the internal erosion resistance of biopolymer-treated soils has been evaluated under full-scale embankment conditions. [7] examined the performance of soils treated with 1% XG through both laboratory and field-scale simulations. The results indicated that 1% XG provided optimal improvements in plasticity and mechanical strength. In full-scale seepage tests beneath a box culvert, untreated embankments collapsed within 1,500 s, whereas XG-treated embankments remained stable up to 2500 s due to enhanced particle bonding, increased apparent cohesion, and pore clogging. These outcomes demonstrate that even low biopolymer dosages can substantially improve embankment durability.

The effectiveness of XG has also been confirmed for highly vulnerable dispersive soils. [8] evaluated the long-term performance of XG-treated dispersive soils subjected to adverse environmental conditions using unconfined compressive strength (UCS) and cyclic wetting-drying tests. Significant strength gains were observed, with UCS increasing by 177% and 95% after 360 days for 2 soil types. After 12 wetting-drying cycles, mass loss values remained below the permissible 14% limit (9.76% and 7.04%), indicating satisfactory durability. So, although cyclic weathering influences strength degradation, XG treatment markedly enhances the long-term stability and erosion resistance of dispersive soils.

Overall, microstructural investigation has become an important approach for understanding the mechanisms of soil stabilization. Quantitative analysis of soil microstructure based on SEM images is increasingly applied in geotechnical research to characterize particle aggregation, pore distribution, and structural densification [9], [10]. Digital image processing tools [11] enable the extraction of geometric parameters, including pore area, particle size, and morphological characteristics from SEM images, allowing a more detailed interpretation of microstructural changes in modified soils.

In this study, SEM images were processed using ImageJ software to quantitatively evaluate the microstructural characteristics of polymer-modified soil. The analysis focuses on parameters describing particle arrangement and structural heterogeneity. Special attention is given to the evolution of particle packing, characteristic diameters (D10, D50, D90), and structural homogeneity under various polymer contents. By linking microstructural metrics with macroscopic behavior, this research provides deeper insight into the mechanisms governing polymer-based soil stabilization.

2. Methods

The soil used in this study was collected from the Astana region, Kazakhstan. It was taken from the subsurface layer at a depth of approximately 0.5-1.0 m, which corresponds to the typical

depth of the engineering soil layer involved in shallow foundation systems and earth structures. The material was air-dried and prepared for laboratory testing under controlled conditions. The particle density of the soil was 2671 kg/m^3 , with a maximum dry density of 1547 kg/m^3 and an optimum water content of 9.61% [12]. Particle size distribution analysis indicated that the soil contains 48% sand, 21% silt, and 31% clay [13]. Based on its granulometric composition, the tested soil is classified as sandy clay loam. The Atterberg limits showed a liquid limit of 19.36% and a plastic limit of 3.17%, resulting in a plasticity index of 16.19%, which reflects moderate plasticity behavior.

XG was selected as the biopolymer additive for soil stabilization in this study. Biopolymer solutions of XG were prepared at concentrations of 3%, 6%, and 9% by weight relative to 100 g of oven-dried soil (hereinafter referred to as XG3, XG6, XG9). Accordingly, 3 g, 6 g, and 9 g of XG were dissolved in distilled water to obtain homogeneous polymer solutions before mixing with the soil. The prepared solutions were then thoroughly blended with the dry soil to ensure uniform distribution of the biopolymer within the soil matrix.

Scanning electron microscopy (SEM) observations were performed using a TM4000Plus scanning electron microscope (Hitachi High-Tech Corporation, Tokyo, Japan). The analysis was carried out under an accelerating voltage of 15 kV in high-vacuum mode using the secondary electron detector to observe the surface morphology of the soil samples.

The preparation process of the sample is presented in Figure 1.



Figure 1 – Sample preparation with polymer mixing and SEM image acquisition

The obtained SEM images served as the foundation for subsequent quantitative image analysis. The acquired micrographs were then imported into ImageJ open software (version 1.53, National Institutes of Health, Bethesda, MD, USA) for quantitative processing. Each image was converted to grayscale and pre-processed using standard noise-reduction and contrast-adjustment steps to improve phase separation. Each SEM image was automatically subdivided into 30 equal regions (each measuring 213×180 pixels) using a standardized grid-based approach implemented in ImageJ. The subdivision was generated programmatically, without manual selection of areas, thereby eliminating operator bias and ensuring reproducible spatial sampling across all samples.

Morphometric analysis was performed independently within each region using the «Analyze Particles» function under identical thresholding parameters for all mixtures. Particle size was quantified using the major axis diameter of detected particles. Size distribution descriptors (D10, D50, and D90) were calculated from the cumulative distribution of measured diameters for each mixture ($n=30$ regions per condition). To quantitatively evaluate microstructural compactness, a densification index (DI) was introduced based on the measured solid area fraction obtained from SEM image analysis. The densification index was defined as:

$$DI = \frac{AF}{1-AF} \quad (1)$$

Where: AF – denotes the solid area fraction expressed as a decimal value; $(1 - AF)$ – represents the corresponding pore fraction.

This ratio characterizes the relative predominance of the solid phase over the void phase within the analyzed microstructure. The solid area fraction (AF) was determined from segmented SEM images using ImageJ software and represents the proportion of the image occupied by soil particles. AF was calculated as:

$$AF = \frac{A_{solid}}{A_{total}} \quad (2)$$

Where: A_{solid} – represents the total projected area of the solid particles identified within the segmented SEM image; A_{total} – denotes the total area of the analyzed field of view.

After grayscale conversion and threshold-based segmentation, binary images were generated to distinguish the solid particle phase from the pore phase. The total analyzed image area (A_{total}) was obtained directly from the image dimensions. This parameter represents the proportion of the microstructural field occupied by the solid phase and serves as a two-dimensional approximation of packing density. A higher DI value indicates that the solid phase occupies a larger proportion of the observed section compared to pores, suggesting a denser particle arrangement. Conversely, lower DI values reflect increased void space and a more open structural configuration.

For each mixture, particle size measurements obtained from the segmented SEM images were statistically processed. The standard deviation (STDV) was calculated to assess the absolute dispersion of particle diameters, while the coefficient of variation (CV) was determined to evaluate the relative heterogeneity of the microstructure. The CV was computed as the ratio of the standard deviation to the mean particle diameter, allowing comparison between compositions with different average particle sizes. All calculations were performed using data extracted from 30 uniformly subdivided image segments.

3. Results and Discussion

SEM micrographs reveal distinct differences in particle arrangement with increasing XG content (Figure 1). The untreated soil exhibits a loose configuration characterized by visible interparticle voids and limited bonding between grains.

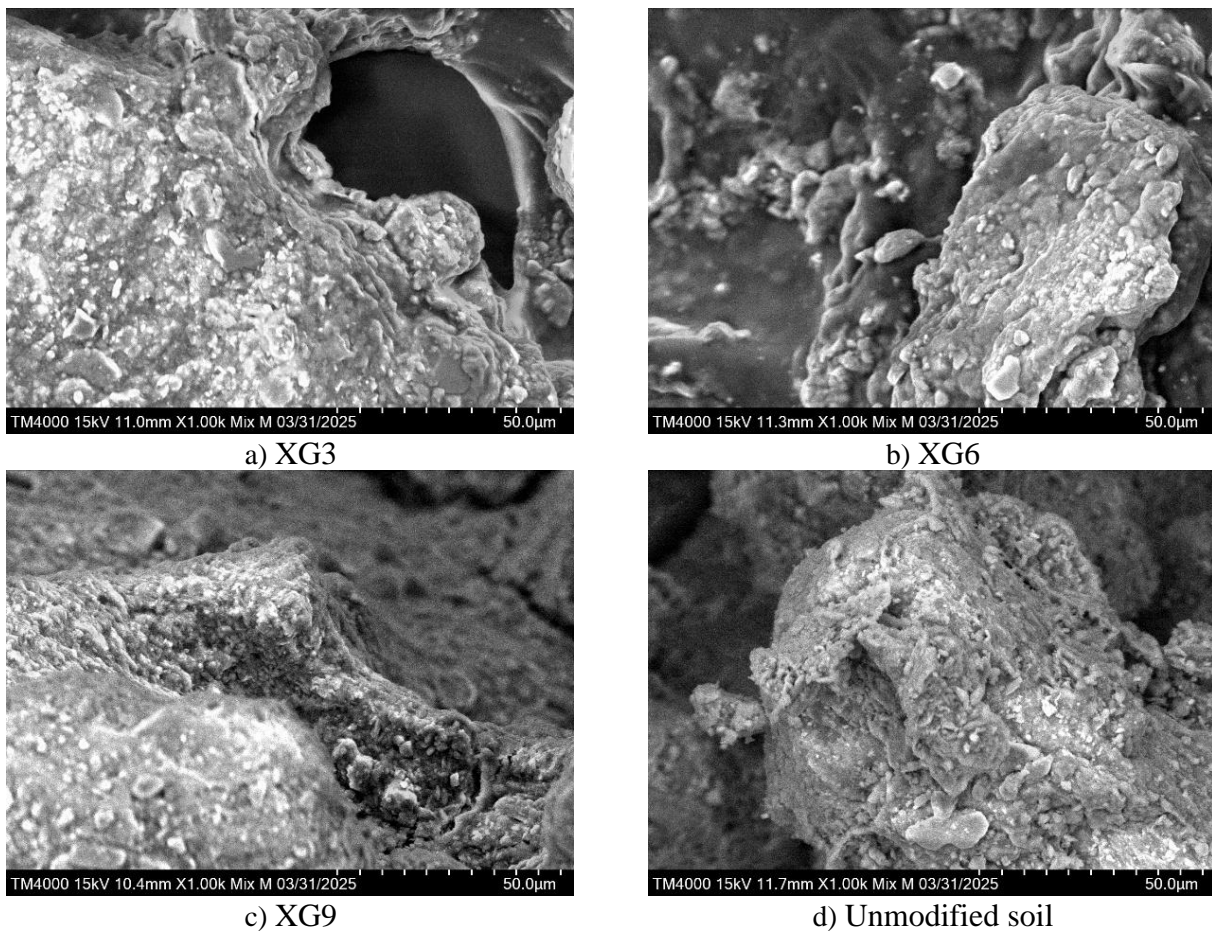


Figure 1 – SEM images of modified soil

At 3% polymer content, a more interconnected structure is observed, with evidence of particle clustering and reduced visible pore space. The 6% sample shows irregular particle distribution with localized dense regions separated by relatively open areas. At 9%, the microstructure appears more heterogeneous, with clustered particle domains and regions of enlarged voids. These visual differences suggest progressive structural modification associated with polymer incorporation.

Binary representations of the SEM images demonstrate clear separation between the solid particle phase and pore spaces across all compositions (Figure 2).

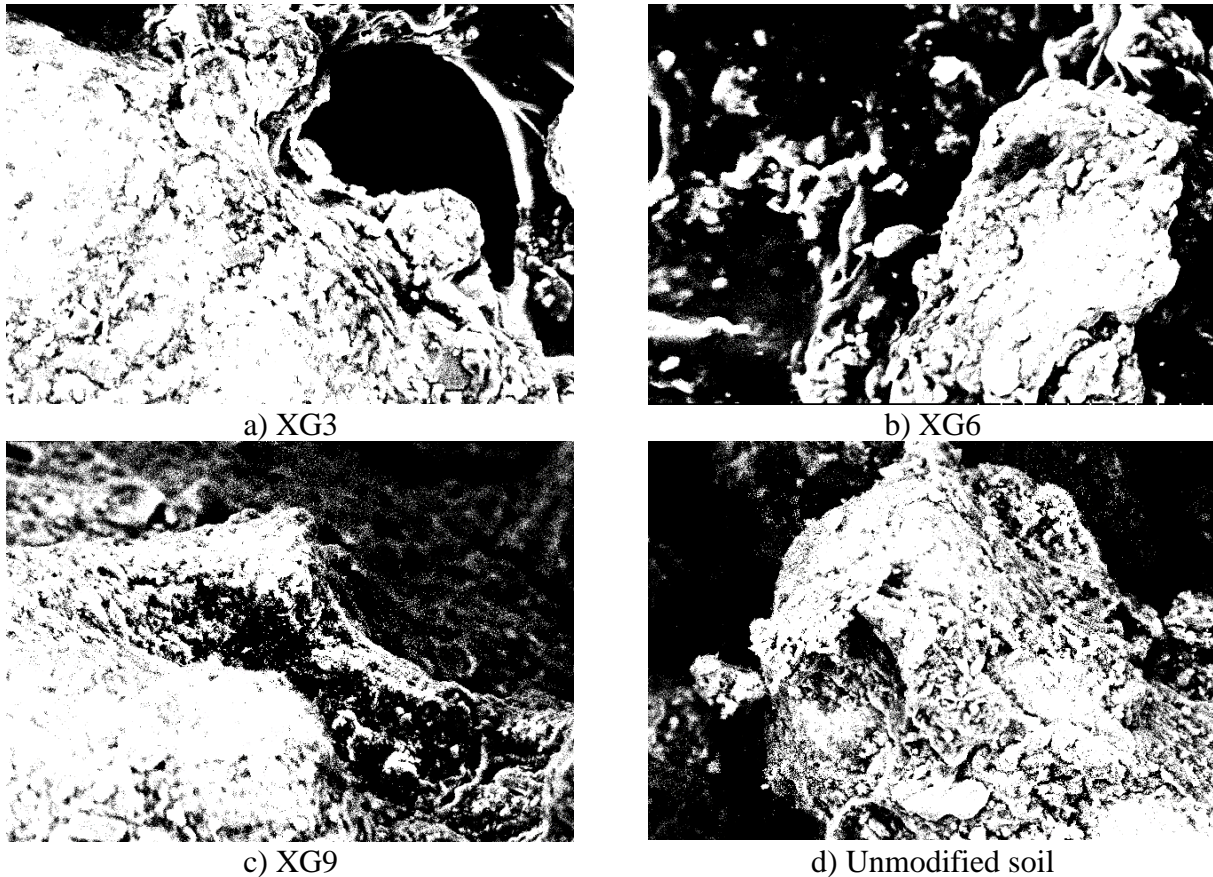


Figure 2 – Binary representations of the SEM images of modified soil

In untreated conditions, dark regions corresponding to voids are more widely distributed throughout the microstructural field. The segmented images provide the basis for quantitative area-based evaluation.

Table 1 presents the microstructural size distribution parameters for untreated and XG-modified soil samples at different polymer contents. The characteristic diameters D10, D50, and D90 reflect the statistical distribution of particle assemblies observed within the SEM field of view.

Table 1 – Microstructural size parameters obtained from SEM image analysis

Polymer content, %	n	D10, μm	D50, μm	D90, μm
0	30	1.925	7.435	8.480
3	30	4.716	7.066	8.605
6	30	4.786	7.326	9.229
9	30	1.770	6.033	8.858

Progressive variation in these parameters indicates that polymer incorporation alters the spatial arrangement of soil particles. In particular, the increase in D50 values with increasing XG content changes the representative structural scale of particle clusters. The differences between D10

and D90 demonstrate shifts in distribution breadth across the tested compositions. These parameters provide a quantitative basis for assessing microstructural modification induced by polymer treatment.

Table 2 summarizes the area-based structural metrics for untreated and XG-modified soil samples.

Table 2 – Derived densification metrics based on SEM area measurements

Polymer content, %	AF	DI
0	0.479	0.92
3	0.575	1.36
6	0.392	0.65
9	0.487	0.95

The solid area fraction (AF) increased from 0.479 in the untreated soil to 0.575 at 3% polymer content, indicating enhanced structural densification at this concentration. This composition exhibited the highest compactness among the tested mixtures.

At 6% polymer content, AF decreased significantly to 0.392, suggesting the formation of additional voids or structural heterogeneity, possibly due to polymer over-saturation. At 9%, the solid fraction partially recovered to 0.487, approaching the value of the untreated soil, which indicates partial structural reorganization rather than further densification (Figure 3).

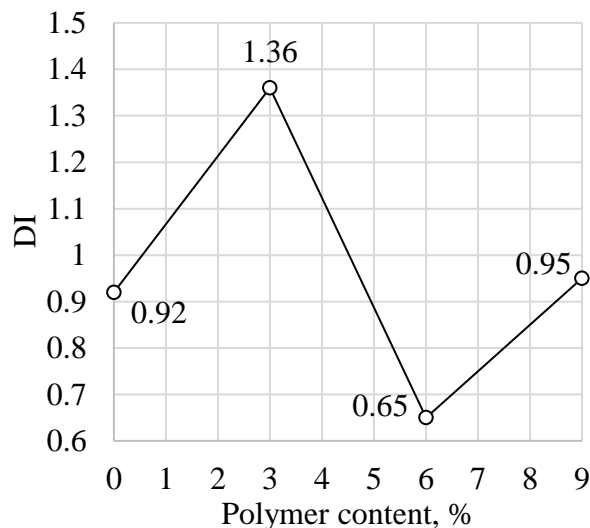


Figure 3 – Variation of densification index with XG content

A similar trend was observed for the densification index. The DI reached its maximum value of 1.36 at 3%, decreased substantially to 0.65 at 6%, and increased again to 9%, although it remained below the peak level. These results indicate a non-linear variation in the solid-to-void relationship with increasing XG dosage. Based on the calculated densification index (DI) values, four structural conditions can be distinguished. The untreated soil (DI = 0.92) represents a discrete particle arrangement characterized by a baseline solid-to-void ratio. A polymer content of 3% (DI = 1.36) produces the most compact structural state, indicating enhanced particle bridging and improved packing efficiency. Increasing the polymer content to 6% leads to a pronounced reduction in the densification index (DI = 0.65), suggesting decreased structural compactness and possible formation of additional voids due to over-saturation or local agglomeration effects. Further increase to 9% results in partial recovery of DI (0.95), approaching the untreated condition. This behavior reflects structural reorganization rather than progressive densification and is consistent with the microstructural heterogeneity observed in SEM images. The statistical dispersion analysis revealed distinct differences in structural variability among the tested polymer contents (Figure 4).

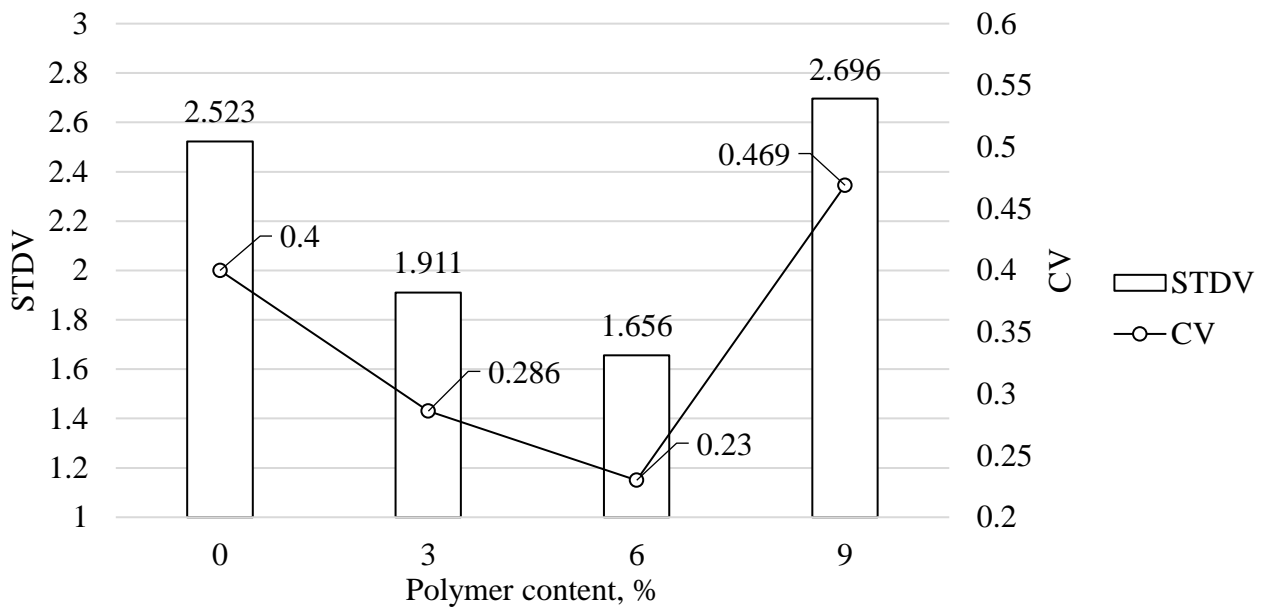


Figure 4 – Variation of particle size dispersion parameters as a function of polymer content

The untreated soil exhibited a standard deviation of 2.523, representing the baseline level of particle size dispersion. The addition of 3% polymer reduced the standard deviation to 1.911, indicating partial structural stabilization. The lowest variability was observed at 6% polymer content (SD = 1.656; CV = 0.230), suggesting the highest degree of microstructural uniformity among the investigated compositions. In contrast, the 9% condition demonstrated a marked increase in dispersion (SD = 2.696), accompanied by the highest coefficient of variation, reflecting structural heterogeneity at elevated polymer dosage.

These results indicate that maximum densification does not necessarily coincide with maximum structural homogeneity. While 3% polymer content yielded the highest compactness according to the densification index, the 6% mixture exhibited the most uniform particle distribution, as reflected by the lowest variability. This suggests that increasing polymer concentration affects not only the degree of particle packing but also the spatial organization of particle assemblies.

The observed microstructural evolution is consistent with trends reported in previous studies on XG-treated soils [14]. Earlier investigations have shown that the improvement of soil properties with increasing XG dosage tends to stabilize after reaching an optimal concentration. For example, studies on silty soils [15] reported that the UCS increased with polymer content but eventually approached a stable state at an optimal dosage of approximately 2%. SEM observations in those studies indicated that XG forms a gel-like matrix that fills pore spaces and enhances the compactness and integrity of the soil structure. These findings are consistent with the present results, where the highest densification was observed at moderate polymer dosage.

In the present study, the formulation of the densification index follows the fundamental concept of solid-void relationships commonly used in soil mechanics, adapted here to a two-dimensional SEM-based framework to enable consistent comparison between samples with different polymer contents.

It should be noted that the present study is limited to SEM-based microstructural evaluation. Therefore, the findings are confined to structural characterization at the microscale. The results contribute to a clearer understanding of dosage-dependent structural transitions in XG-modified soils and provide a quantitative framework for future studies integrating mechanical testing and durability assessment.

Beyond their geotechnical relevance, the obtained results may also support educational applications within digital learning environments. The quantified microstructural transitions identified in this study can be integrated into a soil mechanics module of an educational digital platform, enabling students to explore the relationship between polymer dosage and structural

configuration. The combination of SEM visualization and area-based quantitative metrics provides an effective framework for developing interactive simulation scenarios. Such simulations may allow users to compare untreated and polymer-modified soils, analyze phase distribution patterns, and interpret densification behavior based on measurable parameters.

4. Conclusions

The results demonstrate that polymer dosage significantly influences the internal structure of the soil, leading to a dosage-dependent microstructural evolution. The main findings can be summarized as follows:

1. The untreated soil exhibited a dispersed particle arrangement with clearly distinguishable voids between individual grains. The addition of xanthan gum gradually modified the soil fabric, promoting particle association and altering the connectivity of pore spaces.

2. Binary segmentation analysis revealed distinct changes in the spatial distribution of solid and void phases. Compared with the untreated soil, polymer-treated samples showed increased interaction between soil particles and the biopolymer matrix, although the spatial organization of solid regions varied depending on polymer concentration.

3. Quantitative evaluation of the image-derived parameters indicated a non-linear response of microstructural characteristics to increasing polymer content. Variations in the densification index and phase distribution suggest that different polymer concentrations influence both particles packing and the spatial arrangement of particle clusters.

The results indicate that xanthan gum addition alters both the degree of particle aggregation and the structural organization of the soil matrix. These findings highlight that microstructural densification and structural uniformity may develop differently depending on polymer dosage.

Acknowledgments

This research has been/was/is funded by the Science Committee of the Ministry of Science and Higher Education of the Republic of Kazakhstan (Grant No. AP26195121 «Development of an educational digital platform for future builders with simulation of construction processes and integration with measuring devices via IoT»).

References

- [1] J. Jang, "A Review of the Application of Biopolymers on Geotechnical Engineering and the Strengthening Mechanisms between Typical Biopolymers and Soils," *Advances in Materials Science and Engineering*, vol. 2020, no. 1, p. 1465709, Jan. 2020, doi: 10.1155/2020/1465709.
- [2] A. Tulebekova, Z. Kusbergenova, B. Dosmukhambetova, T. Abilmazhenov, and I. Zhumadilov, "Study of the impact of biopolymer and geosynthetics reinforcement on soil strengthening," *EUREKA: Physics and Engineering*, no. 6, pp. 70–80, Nov. 2024, doi: 10.21303/2461-4262.2024.003472.
- [3] I. Chang *et al.*, "Review on biopolymer-based soil treatment (BPST) technology in geotechnical engineering practices," *Transportation Geotechnics*, vol. 24, p. 100385, Sep. 2020, doi: 10.1016/j.trgeo.2020.100385.
- [4] M. Azimi, A. Soltani, M. Mirzababaei, M. B. Jaksa, and N. Ashwath, "Biopolymer stabilization of clayey soil," *Journal of Rock Mechanics and Geotechnical Engineering*, vol. 16, no. 7, pp. 2801–2812, Jul. 2024, doi: 10.1016/j.jrmge.2023.12.020.
- [5] P. Bagheri, I. Gratchev, and M. Rybachuk, "Effects of Xanthan Gum Biopolymer on Soil Mechanical Properties," *Applied Sciences*, vol. 13, no. 2, p. 887, Jan. 2023, doi: 10.3390/app13020887.
- [6] M. Lee, Y.-M. Kwon, D.-Y. Park, I. Chang, and G.-C. Cho, "Durability and strength degradation of xanthan gum based biopolymer treated soil subjected to severe weathering cycles," *Scientific Reports*, vol. 12, no. 1, p. 19453, Nov. 2022, doi: 10.1038/s41598-022-23823-4.
- [7] Y.-M. Kwon, J.-H. Moon, G.-C. Cho, Y.-U. Kim, and I. Chang, "Xanthan gum biopolymer-based soil treatment as a construction material to mitigate internal erosion of earthen embankment: A field-scale," *Construction and Building Materials*, vol. 389, p. 131716, Jul. 2023, doi: 10.1016/j.conbuildmat.2023.131716.
- [8] J. J. Reddy and B. J. S. Varaprasad, "Long-term and durability properties of xanthan gum treated dispersive soils – An eco-friendly material," *Materials Today: Proceedings*, vol. 44, pp. 309–314, 2021, doi: 10.1016/j.matpr.2020.09.472.

- [9] C.-S. Tang *et al.*, “Quantification and characterizing of soil microstructure features by image processing technique,” *Computers and Geotechnics*, vol. 128, p. 103817, Dec. 2020, doi: 10.1016/j.compgeo.2020.103817.
- [10] N. Ural, “The significance of scanning electron microscopy (SEM) analysis on the microstructure of improved clay: An overview,” *Open Geosciences*, vol. 13, no. 1, pp. 197–218, Feb. 2021, doi: 10.1515/geo-2020-0145.
- [11] G. Di Remigio, I. Rocchi, and V. Zania, “New method for a SEM-based quantitative microstructural clay analysis - MiCA,” *Applied Clay Science*, vol. 214, p. 106248, Nov. 2021, doi: 10.1016/j.clay.2021.106248.
- [12] “GOST 5180-2015 Soils. Laboratory methods for the determination of physical characteristics,” Moscow, Russia: Standartinform, 2015, p. 24.
- [13] “GOST 25100-2020, Soils. Classification,” Moscow, Russia: Standartinform, 2020, p. 38.
- [14] I. Chang, J. Im, A. K. Prasadhi, and G.-C. Cho, “Effects of Xanthan gum biopolymer on soil strengthening,” *Construction and Building Materials*, vol. 74, pp. 65–72, Jan. 2015, doi: 10.1016/j.conbuildmat.2014.10.026.
- [15] X. Zhang, W. Cao, and X. Zhang, “Experimental study on mechanical and hydraulic properties of xanthan gum improved low liquid limit silty soil,” *Scientific Reports*, vol. 14, no. 1, p. 11072, May 2024, doi: 10.1038/s41598-024-61875-w.

Information about authors:

Assel Tulebekova – PhD, Professor, Department of Civil Engineering, L.N. Gumilyov Eurasian National University, Astana, Kazakhstan, azeliyatul@gmail.com

Natalya Ryvkina – Master of Sciences, Senior Lecturer, Department of Civil Engineering, L.N. Gumilyov Eurasian National University, Astana, Kazakhstan, rondv2@mail.ru

Dauren Yessentay – PhD, Associate Professor, Department of Transportation Engineering and Building Materials Production, L.B. Goncharov Kazakh Automobile and Road Institute, Almaty, Kazakhstan, yessentaydauren063@gmail.com

Akmaral Yeleussinova – Candidate of Technical Sciences, Associated Professor, Department of Civil Engineering, L.N. Gumilyov Eurasian National University, Astana, Kazakhstan, yeleussinova70@mail.ru

Author Contributions:

Assel Tulebekova – concept, methodology, testing, modeling, analysis, funding acquisition.

Natalya Ryvkina – concept, editing, funding acquisition.

Dauren Yessentay – resources, data collection, analysis.

Akmaral Yeleussinova – methodology, visualization, interpretation, drafting.

Conflict of Interest: The authors declare no conflict of interest.

Use of Artificial Intelligence (AI): AI were used to assist in literature screening and language refinement. All content was critically reviewed, verified, and edited by the authors to ensure accuracy and scientific integrity.

Received: 16.11.2025

Revised: 10.03.2026

Accepted: 12.03.2026

Published: 12.03.2026



Copyright: © 2026 by the authors. Licensee Technobius, LLP, Astana, Republic of Kazakhstan. This article is an open access article distributed under the terms and conditions of the Creative Commons Attribution (CC BY-NC 4.0) license (<https://creativecommons.org/licenses/by-nc/4.0/>).